AIP | The Journal of Chemical Physics

Benchmarking DFT and semiempirical methods on structures and lattice energies for ten ice polymorphs

Jan Gerit Brandenburg, Tilo Maas, and Stefan Grimme

Citation: The Journal of Chemical Physics **142**, 124104 (2015); doi: 10.1063/1.4916070
View online: http://dx.doi.org/10.1063/1.4916070
View Table of Contents: http://scitation.aip.org/content/aip/journal/jcp/142/12?ver=pdfcov
Published by the AIP Publishing

Benchmarking DFT and semiempirical methods on structures and lattice energies for ten ice polymorphs

Jan Gerit Brandenburg, Tilo Maas, and Stefan Grimme[a)]
Mulliken Center for Theoretical Chemistry, Institut für Physikalische und Theoretische Chemie, Rheinische Friedrich-Wilhelms Universität Bonn, Beringstraße 4, 53115 Bonn, Germany

(Received 2 February 2015; accepted 11 March 2015; published online 26 March 2015)

Water in different phases under various external conditions is very important in bio-chemical systems and for material science at surfaces. Density functional theory methods and approximations thereof have to be tested system specifically to benchmark their accuracy regarding computed structures and interaction energies. In this study, we present and test a set of ten ice polymorphs in comparison to experimental data with mass densities ranging from 0.9 to 1.5 g/cm^3 and including explicit corrections for zero-point vibrational and thermal effects. London dispersion inclusive density functionals at the generalized gradient approximation (GGA), meta-GGA, and hybrid level as well as alternative low-cost molecular orbital methods are considered. The widely used functional of Perdew, Burke and Ernzerhof (PBE) systematically overbinds and overall provides inconsistent results. All other tested methods yield reasonable to very good accuracy. BLYP-D3^{atm} gives excellent results with mean absolute errors for the lattice energy below 1 kcal/mol (7% relative deviation). The corresponding optimized structures are very accurate with mean absolute relative deviations (MARDs) from the reference unit cell volume below 1%. The impact of Axilrod-Teller-Muto (atm) type three-body dispersion and of non-local Fock exchange is small but on average their inclusion improves the results. While the density functional tight-binding model DFTB3-D3 performs well for low density phases, it does not yield good high density structures. As low-cost alternative for structure related problems, we recommend the recently introduced minimal basis Hartree-Fock method HF-3c with a MARD of about 3%. © *2015 AIP Publishing LLC.* [http://dx.doi.org/10.1063/1.4916070]

I. INTRODUCTION

Computationally efficient electronic structure methods are nowadays extensively used in (bio)chemistry, solid state physics, and material science. In this regard, density functional theory (DFT) has emerged as "work horse" for many applications and is still an active research field of general interest.[1] DFT provides an excellent compromise between accuracy and computational cost. Even more efficient semiempirical methods have gained an increased importance for large scale screenings of numerous conformers and in the field of molecular dynamics beyond the classical force field approximation. However, both semi-local DFT and semiempirical approximations thereof are not capable of describing long-range electron correlation effects leading to the important London dispersion interactions.[2] In the last decade, this flaw and its correction was an intense research topic and an explicit account of London dispersion is now standard in DFT and semiempirical frameworks.[3–5] For further details on these methods, we refer to Refs. 6 and 7 with some review character.

Water in its various phases is of utmost importance in biological systems.[8] The special physical chemistry of water systems covers thermodynamical properties, critical phenomena, and chemical reactions.[9] Theoretical methods shall help and guide experimentalists in this regard which requires an accurate treatment of the various condensed phases of water. This primarily involves the description of (mostly non-covalent) interaction energies and resulting structures. Recently, some efforts were undertaken to perform relatively high-level MP2 and random phase approximation (RPA) (energy and gradient) calculations of liquid water and ice, but these are presently only possible with huge computational resources.[10] Especially, the dynamics of biomolecules in water and of water at solid surfaces is an active research field with many challenges.[11]

Because DFT and semiempirical methods by construction contain some empirical elements, their careful benchmarking is mandatory. In the past, most DFT benchmarks focused on isolated molecules, dimers, and small clusters (e.g., Refs. 12–14). Presently, only one common benchmark set for organic solids exists.[15] In this so-called X23 set, only two polymorphs are included and systems with strong hydrogen bonds are under-represented. Previous studies investigated some ice polymorphs with mostly PBE based density functionals (DFs) with and without corrections for London dispersion effects.[16] Recently, Kresse and coworkers applied RPA to various ice modifications, and for some structures, embedded many-body expansions at the "gold standard" coupled-cluster single double (triple) (CCSD(T)) level have been used .[17]

In the present study, we investigate a selection of ten experimentally studied ice polymorphs. The performance of various DFs at the generalized gradient approximation (GGA),

a)Electronic mail: grimme@thch.uni-bonn.de

meta-GGA, hybrid, and (range separated) hybrid level is investigated. Both the structure and corresponding lattice energy are analyzed. Additionally, some low cost molecular orbital (MO) based methods which showed promising accuracy previously[7] are tested. Furthermore, the importance of an accurate treatment of London dispersion even in systems dominated by hydrogen-bonding is highlighted.

We first present the ten ice polymorphs under consideration with the experimental references in Sec. II A. Section II B shortly summarizes the computational details. We correct the X-ray structures for zero-point and thermal effects as described in Sec. II C. The main results of this study are given in Sec. III, separated into a potential surface analysis of the high density ice VIII (Sec. III A), a structure benchmark (Sec. III B), a lattice energy benchmark (Sec. III C), and a comparison to results for gas phase water clusters (Sec. III D). Finally, a conclusion with recommended methods is given in Sec. IV.

II. BENCHMARK SETUP

A. Systems under consideration

We have compiled the ICE10 set by combining ten different ice polymorphs as summarized in Table I. Their structures were determined by low temperature neutron diffraction experiments. The systems contain 8–28 water molecules per crystal unit cell and all obey the "ice rules" (Bernal-Fowler rules).[18] We consider four proton ordered and six proton disordered systems. The proton ordered crystals typically occur at higher densities, where the hydrogens are at fixed positions with low entropy. The unit cell volumes (per molecule) vary between 18 and 32 Å^3. Because the experimental detection and accurate placement of hydrogen atoms is challenging, we use the theoretical unit cell volume (which corresponds to a certain mass density) as most sensitive and reliable structure quality criterion. The sublimation enthalpies of systems 1-7 were determined experimentally and extrapolated to electronic (zero-point vibrational exclusive) lattice energies at 0 K. These reference energies can be directly compared to the calculated ones in order to judge the quality of a theoretical method. For systems 7-10, no experimental sublimation data are available. We give theoretical estimates in Table I at our "best" theoretical level, which can be used as reference for methods at a lower theoretical level like GGA density functionals, small basis set calculations, or semiempirical methods.

In Figure 1, we show a single unit cell for each crystal. One can see the variety of different hydrogen bond networks with proton ordered conformations and proton unordered structures. Table I summarizes all important properties of the ten crystals. When multiple experimental data are available, we give both volumes and mass densities and use the latest published values in comparisons with theory.

B. Computational details

The DFT calculations are mostly conducted with the VASP program package.[27] The projector augmented plane-wave method (PAW) is used with hard pseudo-potentials constructed by Blöchl and Kresse.[28] In order to approach the basis set limit, a huge PAW energy cutoff of 1000 eV is used. Detailed convergence tests showed that this is required in unconstrained geometry optimizations. In smaller basis sets, artificial Pulay stress can lead to too small unit cell volumes. For instance, an optimized Ih structure with PAW cutoff of 600 eV has a 2% smaller unit cell compared to the 1000 eV basis set calculation. That the basis set limit is indeed reached was confirmed by a corresponding potential energy scan. Similar effects have been observed before in organic crystals.[29] In the following, the 1000 eV PAW basis is used if not mentioned otherwise.

We apply several GGA functionals (PBE,[30] RPBE,[31] revPBE,[32] and BLYP[33]), the meta-GGAs TPSS[34] and M06L,[35] two global hybrid functionals (PBE0[36] and B3LYP[37]), and the range-separated hybrid functional HSE06.[38] Because of the significantly higher computational demands, the hybrid functionals are only used for single-point energy calculations. The single-point energy calculations were consistently done on the PBE-D3 structures. The non-covalent geometries are typically less sensitive to the inclusion of Hartree-Fock exchange compared to the impact on the lattice energy. Though some functionals are shown to yield better geometries, we choose the PBE-D3 level. This is the standard procedure conducted by our group, and it is consistent with other approaches, e.g., Tkatchenko and coworkers calculate the PBE0-MBD energies on PBE-Tkatchenko-Scheffler (PBE-TS) geometries.[15,16]

Though ice forms complex networks of hydrogen bonds with large electrostatic and induction contributions to the binding energy, London dispersion forces cannot be neglected. In order to investigate its importance, all methods are applied with and without the D3 London dispersion correction.[3] It is applied in the most recent Becke-Johnson damping variant.[39] Only M06L is used with the zero damping scheme (denoted by D3(0)) to minimize the double counting of short-range dispersion effects, which are covered by the meta-GGA. For final single point energies, our standard three-body dispersion term (of Axilrod-Teller-Muto (ATM) type[40]) is included and will be indicated by the superscript atm.

Due to the increased importance of low-cost methods as a bridge between first-principles DFT and classical force fields, some alternative approaches are tested as well. We conduct plain B3LYP/6-31G* calculations with atom-centered Gaussian basis sets of double-zeta quality with the CRYSTAL14 program.[41] Additionally, a minimal basis set Hartree-Fock approach with corrections for dispersion (D3), basis set superposition error (gCP[42]), and short-range basis set error (SRB), dubbed HF-3c, is applied.[43] HF-3c frequencies are scaled by 0.86 as suggested in its original publication.

As the computationally fastest here considered method, the dispersion corrected density functional tight-binding DFTB3-D3[44,45] is applied. We use the latest third order version with empirical damping of hydrogen containing pair-potentials and self-consistent charge redistribution as implemented in dftb+.[46] The 3OB Slater-Koster files constructed by Elstner and coworkers are used.[47] The latter two methods showed an excellent performance on benchmark sets for general non-covalent interactions.[7] The D3, gCP, and

TABLE I. Systems contained in the ICE10 benchmark set. Crystallographic specifications, experimental densities (measured at temperature T_{exp}), and lattice energies extrapolated to 0 K are given.

No.	Polymorph	#H_2O	Bravait lattice	Spacegroup	Protons[a]	T_{exp}	Vol.	ρ	E_{lat}
1	Ih[19]	16	Hexagonal	$P6_3/mmc$	Disordered	10	32.05, 32.50	0.93, 0.92	14.07
2	II[20]	12	Rhombohedral	$R\bar{3}$	Ordered	0	24.97, 24.63	1.20, 1.21	14.05
3	III[21]	12	Tetragonal	$P4_12_12$	Disordered	90	25.69	1.16	13.85
4	VI[22]	10	Tetragonal	$P4_2/nmc$	Disordered	98	22.84	1.31	13.68
5	VII[21]	16	Cubic	$Pn\bar{3}m$	Disordered	90	20.26	1.48	13.07
6	VIII[23]	8	Tetragonal	$I4_1/amd$	Ordered	0	20.09, 18.61	1.49, 1.61	13.31
7	IX[24]	12	Tetragonal	$P4_12_12$	Ordered	30	25.63, 25.80	1.17, 1.16	13.97
8	XIII[25]	28	Monoclinic	$P2_1/a$	Ordered	80	23.91	1.25	13.95[b]
9	XIV[25]	12	Orthorhombic	$P2_12_12_1$	Ordered	80	23.12	1.29	13.74[b]
10	XV[26]	10	Tetragonal	P1	Ordered	80	22.45	1.33	13.48[b]

[a]Unit cell volume per molecule is given in $Å^3$, molecular mass density in g cm^{-3}, lattice energy (at 0 K) in kcal mol^{-1}, and temperature in K.
[b]Theoretical estimate at the PBE0-D3^{atm} level with removed systematic shift.

HF-3c methods are implemented in a CRYSTAL14 developer version and will be generally available in its next release.

The Brillouin zone is sampled with dense k grids of approximately 0.02 $Å^{-1}$ generated via the Monkhorst-Pack scheme. The Γ-centered number of k-points is given in the supplementary material.[48] Structures are fully optimized without symmetry constraints until all forces are below 0.005 eV/Å. Especially for flat potential energy surfaces (PESs), tight convergence thresholds are necessary.[49] In the PAW calculations for a single (isolated) water molecule, a large unit cell (12 Å) is employed to minimize the interaction with its periodic images.

C. Correction for zero-point energies

The measurements of structure and lattice energy have been conducted at finite temperature (up to 100 K). The experimental lattice energies provided by Whalley were extrapolated to 0 K and zero-point vibrational energies (ZPVEs) have been removed.[21] The accuracy of the extrapolated energies has been verified by high-level diffusion quantum Monte Carlo (DMC) and embedded many-body CCSD(T) calculations.[17,50] We further assume that the thermal contribution to the ice density (from 0 to 98 K) is rather small, and the measured structure can be treated as equilibrium (R_e) geometry as discussed further below.

However, the ZPVE is substantial and cannot be neglected. In order to provide an easy usable benchmark, we estimate its effect on the unit cell volume (and the mass density, respectively) for all ten systems. For each system, we perform constrained (constant volume) optimizations around the electronic equilibrium geometry with scaled unit cell volumes of $80\%V_e$, $90\%V_e$, $95\%V_e$, $100\%V_e$, $105\%V_e$, $110\%V_e$, $120\%V_e$, and $130\%V_e$. On these optimized structures, the vibrational frequencies are computed in the harmonic approximation. The ZPVE together with the Bose-Einstein

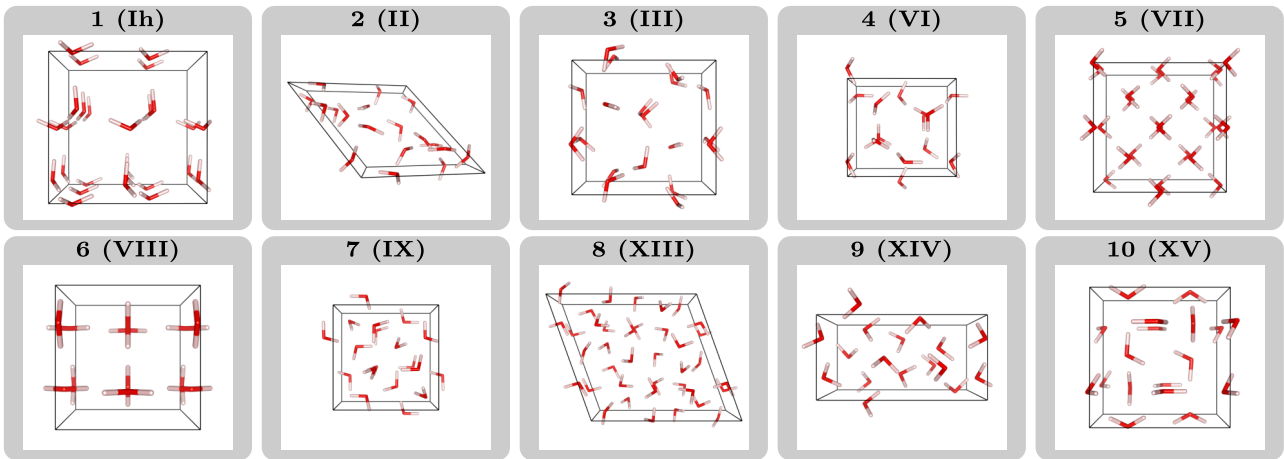

FIG. 1. Systems contained in the ICE10 benchmark set. The perspective projection of a single unit cell is shown.

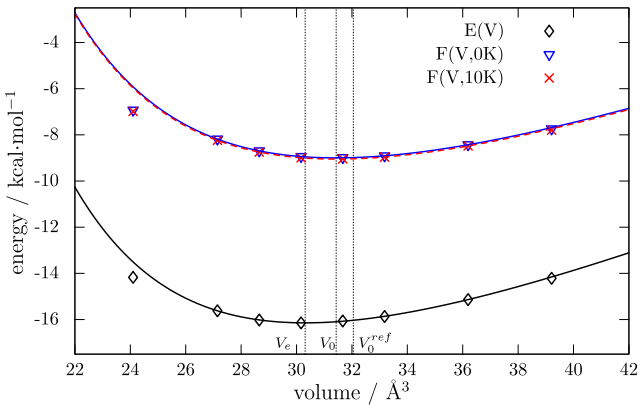

FIG. 2. Electronic energy surface $E(V)$ and free energy surface $F(V)$ on the HF-3c level for the ice Ih polymorph compared to the experimental volume V_0^{ref}. The free energy F includes zero-point and thermal contributions in the harmonic approximation.

occupied phonon modes leads to the free energy,

$$F(V) = E(V) + \sum_q \left(\frac{\hbar\omega_q(V)}{2} + \frac{\hbar\omega_q(V)}{e^{\frac{\hbar\omega_q(V)}{k_B T}} - 1} \right). \quad (1)$$

The phonon modes with frequencies $\omega_q(V)$ depend on the volume V. Therefore, the correction to the electronic energy also depends on the volume. To the data points $F(\{V_i\})$ and $E(\{V_i\})$, we fit a Murnaghan equation of state,

$$E, F(V) = E_{e,0} + \frac{B_{e,0}V}{B'_{e,0}(B'_{e,0} - 1)} \times \left(B'_{e,0}\left(1 - \frac{V_{e,0}}{V}\right) + \left(\frac{V_{e,0}}{V}\right)^{B'_{e,0}} - 1 \right), \quad (2)$$

and extract the equilibrium volumes V_e and the free energy volumes V_0. The bulk modulus B and its derivative B' are not further analyzed.

As shown below, the HF-3c method provides very reasonable potential energy surfaces at rather low computational costs. This makes it an ideal choice for the free energy calculations. Therefore, the total energy E_{tot}(V) in the above scheme is evaluated at the HF-3c^{atm} level (ATM three-body term included). In order to judge the accuracy of this HF-3c based back-correction, we compare it for system Ih and VIII with values from Murray and Galli.[51] They calculate vibrational corrections to the volume at the vdW-DF2 level of 1.9% and 5.8%, respectively. The deviation to the corresponding HF-3c corrections (3.6% and 5.1%) is rather small. While they also compute PBE based corrections, we believe that the comparison to the apparently wrong PBE potential (see below) should be avoided. Because the two examples cover both extremes (high and low densities) of the ice phases, we expect the results to be transferable to the other systems. In our experience, the steepness of the intermolecular DFT potential typically increases with higher HF exchange, which is systematically removed by the frequency scaling. The HF-3c potential energy surface (PES) of ice Ih is shown in Figure 2.

Apparently, the equation of state is a good model around the equilibrium. The ZPVE has two effects. First, it shifts the minimum to higher energies by approximately 8 kcal/mol. Additionally, the free energy minimum occurs at ≈4% larger unit cell volume. Compared to the significant ZPVE effect, the impact of the three-body dispersion (ATM) term is with 0.3% rather small. The impact of the thermal-vibrational contributions at these low temperatures is tiny (<0.1%) and the construction of a large supercell for the phonon calculation is not necessary. The unit cell volume extracted from the free energy surface V_0 is very close to the experimental value with a deviation below 2%.

In Table II, we summarize the equilibrium volumes calculated by HF-3c together with the measured volumes V_0 and the "experimental" equilibrium volumes V_e^{ref}. If different experimental measurements are available, we use the latest published values (first value given for volume and density in Table I). We propose the back-corrected volumes V_e^{ref} as reference benchmark values, which can be compared to free optimizations on the electronic energy surface. The increase of the volume due to free energy contributions is on average 3.7% with a standard deviation of 1.0%. We observe an increased correction with increasing density (linear correlation with correlation coefficient $R^2 = 0.7$), which is expected. However,

TABLE II. Correction of equilibrium volumes V_e to free-energy volumes V_0 due to ZPVE and thermal energies calculated at the HF-3c^{atm} level.

	Theory[a]			Experiment[b]		
No.	V_0	V_e	$\Delta V/V_0$ (%)	V_0	V_e^{ref} (±1.2%)	ρ_e^{ref}
1	31.43	30.31	3.6	32.05	30.91	0.96
2	24.67	23.68	4.0	24.97	23.97	1.25
3	26.97	26.55	1.6	25.69	25.29	1.18
4	21.85	21.03	3.8	22.84	21.98	1.36
5	18.86	17.96	4.8	20.26	19.28	1.55
6	18.93	17.96	5.1	20.09	19.06	1.57
7	25.81	25.14	2.6	25.63	24.97	1.20
8	23.29	22.43	3.7	23.91	23.03	1.30
9	22.56	21.72	3.7	23.12	22.26	1.34
10	22.01	21.15	3.9	22.45	21.58	1.38

[a]Volumes given in Å^3 and densities in g/cm^3.

[b]Experimental V_e estimated as $V_e^{ref} = V_0^{ref}\left(1 + \frac{V_e^{calc} - V_0^{calc}}{V_0^{calc}}\right)$ with V^{calc} at the HF-3c level.

this is only a rough trend, and the specific volume expansion depends non-trivially on the geometry.

III. RESULTS AND DISCUSSION

A. Potential energy surface of ice VIII

We first investigate the potential energy landscape of the high density ice polymorph VIII in some detail. We calculate the electronic PES by scaling the lattice vectors of the minimum geometry and performing a constraint volume optimization as described in the previous paragraph. This illustrative example is shown in Figure 3 for PBE, PBE-D3, RPBE-D3, revPBE-D3, TPSS-D3, TPSS-D3^{atm}, HF-3c^{atm}, and DFTB3-D3^{atm} to demonstrate the typical behavior of these methods. For an easier comparison, we show in each plot the PBE and PBE-D3 potentials for comparison.

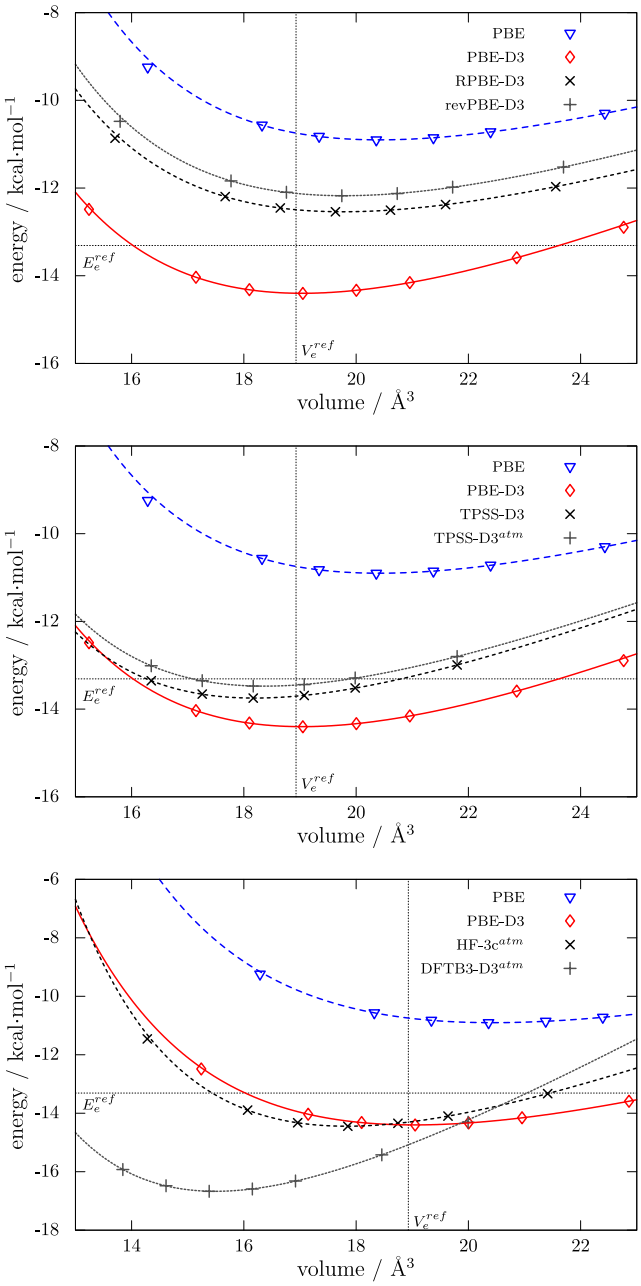

FIG. 3. Electronic energy surface of the ice VIII polymorph on various theory levels compared to the experimental references. Zero-point and thermal effects are explicitly excluded from the reference energy E_e^{ref} and reference volume V_e^{ref}.

The minima of all methods determined via the PES fit agree well with the free optimizations. Especially for the calculations in the PAW basis, this is an important test for basis set completeness and the applied geometry convergence criteria. Plain PBE gives significantly too large lattice parameters resulting in an unit cell volume which is overestimated by 7%. The corresponding lattice energy of 10.9 kcal/mol is too small by 2.4 kcal/mol. The D3 dispersion correction leads to much better structures, i.e., the unit cell volume of PBE-D3 deviates from the reference by less than 0.2%. However, the minimum is significantly too low (overestimated lattice energy). The PBE functional is known to overestimate hydrogen bonding[52] which is very pronounced in the ice crystals with many strong hydrogen bonds. The physically correct inclusion of London dispersion lowers the energy further and leads to the observed effect. The revised versions RPBE and revPBE were constructed to give more reasonable energies for these kind of systems. Both potentials are rather similar. The lattice energy is indeed improved (error of RPBE-D3 below 1 kcal/mol). However, the minimum corresponds to a by 3.7% too large unit cell. The behavior that revPBE sometimes deteriorates the good PBE structures was already recognized by the authors of PBE for covalent bonding.[53] Of all PBE variants and successors, respectively, TPSS-D3 performs best with accurate and consistent lattice energy and structure. The inclusion of the ATM term has small effects, but overall improves the results. For the geometries, we estimate the three-body contribution by a potential energy scan (see Sec. II C) and scale the corresponding TPSS-D3 unit cell volumes. The lattice energy of TPSS-D3^{atm} deviates by only 0.2 kcal/mol from the reference and the cell is 3.6% too small, which we consider reasonably good. Interestingly, the internal structures of covalently bound, medium-sized molecules are systematically too large at the TPSS-D3 level, and this also holds for the X23 set of molecular crystals.[14,53] Apparently, this cannot be directly transferred to the ice phases where the density mainly depends on the non-covalent hydrogen bond lengths.

The computational cost of all non-hybrid DFT methods is practically identical, and only the meta-GGA TPSS is slightly more expensive than the GGAs. Two low cost methods, namely, HF-3c and DFTB3-D3, are included in Figure 3. In the HF-3c method, the Hartree-Fock part is evaluated in a minimal GTO basis set, which leads to a speed-up of ≈50 compared to the DFT/PAW calculations. Notably, however, the corresponding PES is close to the reference. The lattice energy is overestimated by 1.1 kcal/mol and the unit cell is by 6.4% too small. Especially, the good structure and reasonable PES shape is important for the low-cost methods which are often used for geometry optimization and frequency calculations. In the tight-binding model DFTB3, no three- and four-center integrals have to be evaluated. This yields an additional speed up of two orders of magnitude compared to HF-3c but on the other hand introduces some significant errors. The important many-center contributions are missing,

which leads to a wrong repulsive potential, especially at high densities. The lattice energy is overestimated, but the deviation of 3.4 kcal/mol is acceptable. The system specific results discussed so far are supported by the statistical analysis of the whole ICE10 benchmark set given in Secs. III B and III C.

B. Equilibrium structures for ICE10

In the following, we analyze the equilibrium structures of the full ICE10 benchmark set. Correct structures are in general important for the application of more involved electronic structure methods. For instance, an embedded cluster approach with high-level correlated wavefunction methods relies on accurate input geometries. Especially for localized correlation methods, analytical gradients are not feasible and therefore good DFT structures are needed. The ICE10 systems are all optimized with the (meta-)GGA density functionals and the three low-cost methods. Note that the optimization with a hybrid functional in a nearly complete PAW basis is currently not feasible on standard work stations. Optimizations with the meta-GGA M06L are not performed because of numerical problems (SCF convergence).

In Table III, the experimental and theoretical unit cell volumes are summarized. We additionally give the mean relative deviation (MRD) and the mean absolute relative deviation (MARD) with respect to the reference using 10 data points. For selected methods, we show a graphical representation of the unit cell volume in Figure 4.

All plain semi-local density functional approximations (PBE, RPBE, revPBE, BLYP, and TPSS) produce significantly too large volumes with MARDs ranging from 4% to 24%. The behavior of the PBE variants is very different, though their mathematically similar functional form. Inclusion of the D3 dispersion correction clearly improves the results and all MARDs are below 4%. This demonstrates the importance of long-range London dispersion effects even though a significant contribution to the binding in ice is due to electrostatic and induction effects. Interestingly, the PBE-D3 volumes are underestimated, while the revised PBE variants overestimate them. The effect of including the three-body dispersion is rather small, but on average improves the results. In general, all dispersion corrected density functionals evaluated in a large PAW basis set can be recommended. BLYP-D3^{atm} performs exceptionally good with a MARD of only 1% without systematic shift. This is in agreement with recent results for the properties of liquid water.[54]

However, the PAW based free optimizations can be computationally expensive. Therefore, we tested the low-cost methods introduced in the previous paragraph. Somewhat surprisingly, B3LYP in a small 6-31G* basis set performs well. This is due to an error compensation between the missing long-range London dispersion and the artificial basis set superposition error.[55] The good result for the ice crystals

TABLE III. Comparison of calculated unit cell volumes of the ICE10 benchmark set with the experimental reference.

	1	2	3	4	5	6	7	8	9	10	MRD	MARD[a]
Expt. reference (V_e^{ref})	30.9	24.0	25.3	22.0	19.3	19.1	25.0	23.0	22.3	21.7	...	...
DFT												
PBE	30.2	24.5	26.4	22.3	20.4	20.4	26.2	23.6	22.9	22.4	3.1	3.6
RPBE	33.7	29.0	30.5	26.9	26.2	26.2	30.2	28.0	27.4	27.0	23.7	23.7
revPBE	33.1	28.0	29.8	25.9	24.6	24.5	29.8	27.1	26.4	26.0	19.1	19.1
BLYP	32.2	26.3	29.0	23.9	22.0	22.0	27.5	25.3	24.5	24.1	10.9	10.9
TPSS	30.5	24.8	26.7	22.5	20.0	19.9	27.0	23.9	23.2	22.6	3.9	4.1
DFT-D												
PBE-D3	29.1	23.2	24.4	20.9	18.9	19.1	24.1	22.2	21.5	21.1	−3.2	3.2
RPBE-D3	30.6	24.4	25.6	22.0	19.7	19.6	25.4	22.2	22.6	22.1	1.0	1.8
revPBE-D3	30.4	24.2	25.4	21.7	19.7	19.7	25.3	23.1	22.3	21.8	0.7	1.3
BLYP-D3	30.4	23.9	24.9	21.4	19.4	19.4	24.5	22.8	22.0	21.5	−0.8	1.3
TPSS-D3	29.3	23.2	24.6	20.8	18.2	18.2	24.5	22.2	21.5	21.0	−3.8	3.8
DFT-D^{atm}												
PBE-D3^{atm}	29.2	23.3	24.6	21.0	19.0	19.2	24.3	22.4	21.6	21.2	−2.7	2.8
RPBE-D3^{atm}	30.7	24.6	25.8	22.1	19.8	19.8	25.6	22.4	22.7	22.2	1.6	2.3
revPBE-D3^{atm}	30.5	24.3	25.7	21.9	19.9	19.8	25.5	23.2	22.4	22.0	1.3	1.7
BLYP-D3^{atm}	30.5	24.0	25.2	21.5	19.5	19.5	24.7	22.9	22.1	21.6	−0.3	1.0
TPSS-D3^{atm}	29.4	23.3	24.8	21.0	18.3	18.3	24.7	22.4	21.6	21.1	−3.2	3.2
Low-cost												
B3LYP/6-31G*	30.1	23.7	24.9	21.3	19.1	19.1	24.7	22.9	21.9	21.4	−0.5	2.1
HF-3c^{atm}	30.1	23.6	26.5	21.0	18.0	18.0	25.0	22.4	21.7	21.1	−2.4	3.3
DFTB3-D3^{atm}	30.1	21.8	18.7	18.7	15.5	15.5	20.6	19.4	19.4	18.6	−15.1	15.1

[a]Volumes are given in Å^3. Mean relative deviations (MRDs) and mean absolute relative deviations (MARDs) are given in %.

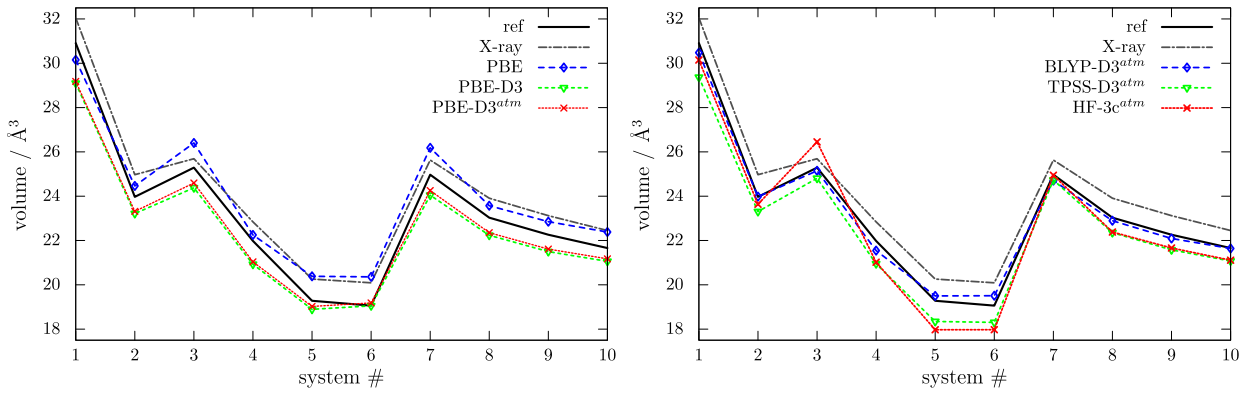

FIG. 4. Unit cell volume in Å^3 of the ten ice polymorphs for selected methods compared to the reference. Note the significant deviation between the raw X-ray data and the back-corrected reference values.

cannot be generally transferred to other systems. For instance, plain B3LYP in a similar SVP basis set was shown to perform badly on various molecular crystals.[42] HF-3c is evaluated in an even smaller minimal basis set but performs only slightly worse compared to the dispersion corrected functionals. The MARD is only 3.3% and at the same time a speed up of 50–100 is achieved compared to the TPSS-D3/PAW calculations. We have recently shown that the combination of the DFTB3 model with the D3 correction can describe various organic molecular crystals reasonably well.[45] Unfortunately, the geometries of the ice crystals are not satisfactory. The volumes are on average too small by 15%, and the largest errors occur for the high density phases. Only the structure of the most stable low density ice Ih can be reproduced with DFTB3-D3 to

TABLE IV. Comparison of calculated lattice energies of the ICE10 benchmark set to the experimental reference.

	1	2	3	4	5	6	7	8	9	10	MD	MAD[a]
Expt. reference (E_{lat}^{ref})	14.1	14.1	13.9	13.7	13.1	13.3	14.0	…	…	…	…	…
DFT												
PBE	15.3	13.5	14.1	12.6	10.9	10.9	14.2	13.3	14.0	12.6	−0.6	1.1
RPBE	11.3	9.4	10.2	8.6	6.8	6.8	10.3	9.3	9.0	8.5	−4.7	4.7
revPBE	11.5	9.5	10.3	8.5	6.7	6.7	10.4	9.3	8.9	8.5	−4.7	4.7
BLYP	12.8	10.8	11.5	9.9	8.0	8.0	11.5	10.6	10.3	9.8	−3.3	3.3
TPSS	14.0	11.9	12.6	10.9	9.1	9.1	12.8	11.7	11.3	10.8	−2.2	2.2
M06L	11.2	12.0	11.6	12.4	13.5	13.4	11.6	12.0	12.2	12.3	−1.5	1.6
DFT-D												
PBE-D3	17.4	16.3	16.6	15.7	14.4	14.4	16.7	16.2	16.0	15.6	2.2	2.2
RPBE-D3	15.1	14.1	14.4	13.7	12.5	12.5	14.5	14.0	13.9	13.6	0.1	0.5
revPBE-D3	15.2	14.4	14.6	14.0	12.8	12.8	14.7	14.3	14.1	13.9	0.4	0.6
BLYP-D3	15.9	15.2	15.3	14.8	13.7	13.7	15.5	15.1	15.0	14.7	1.1	1.1
TPSS-D3	16.4	15.2	15.6	14.7	13.5	13.4	15.7	15.1	14.9	14.6	1.2	1.2
M06L-D3(0)	12.0	12.9	12.5	13.3	14.6	14.5	12.5	13.0	13.1	13.3	−0.5	1.3
DFT-D^{atm}												
PBE-D3^{atm}	17.2	16.1	16.4	15.5	14.2	14.2	16.5	16.0	15.8	15.4	2.0	2.0
RPBE-D3^{atm}	15.0	14.0	14.3	13.5	12.3	12.3	14.4	13.8	13.7	13.4	0.0	0.6
revPBE-D3^{atm}	15.1	14.2	14.5	13.8	12.6	12.6	14.6	14.1	13.9	13.7	0.2	0.5
BLYP-D3^{atm}	15.8	15.0	15.2	14.6	13.4	13.4	15.3	15.0	14.8	14.5	1.0	1.0
TPSS-D3^{atm}	16.3	15.1	15.4	14.4	13.2	13.2	15.6	15.0	14.7	14.4	1.0	1.1
M06L-D3(0)^{atm}	11.9	12.7	12.3	13.1	14.3	14.2	12.4	12.8	12.9	13.1	−0.7	1.3
DFT-D^{atm} Hybrid												
PBE0-D3^{atm}	15.8	14.9	15.0	14.4	13.4	13.3	15.2	14.8	14.6	14.3	0.8	0.8
B3LYP-D3^{atm}	15.5	14.9	14.9	14.5	13.6	13.6	15.1	14.8	14.7	14.4	0.8	0.8
HSE06-D3^{atm}	15.7	14.9	15.2	14.4	13.3	13.3	15.4	14.9	14.6	14.4	0.9	0.9
Low-cost												
B3LYP/6-31G*	21.1	20.2	20.5	19.7	18.1	18.1	20.5	18.3	19.9	19.6	6.0	6.0
HF-3c^{atm}	16.0	15.3	15.3	14.6	14.2	14.2	15.6	15.2	14.8	14.6	1.3	1.3
DFTB3-D3^{atm}	13.4	14.4	14.9	14.7	16.7	16.7	14.4	14.7	14.5	14.9	1.3	1.5

[a]Energies, mean deviations (MDs) and mean absolute deviations (MADs), are given in kcal/mol.

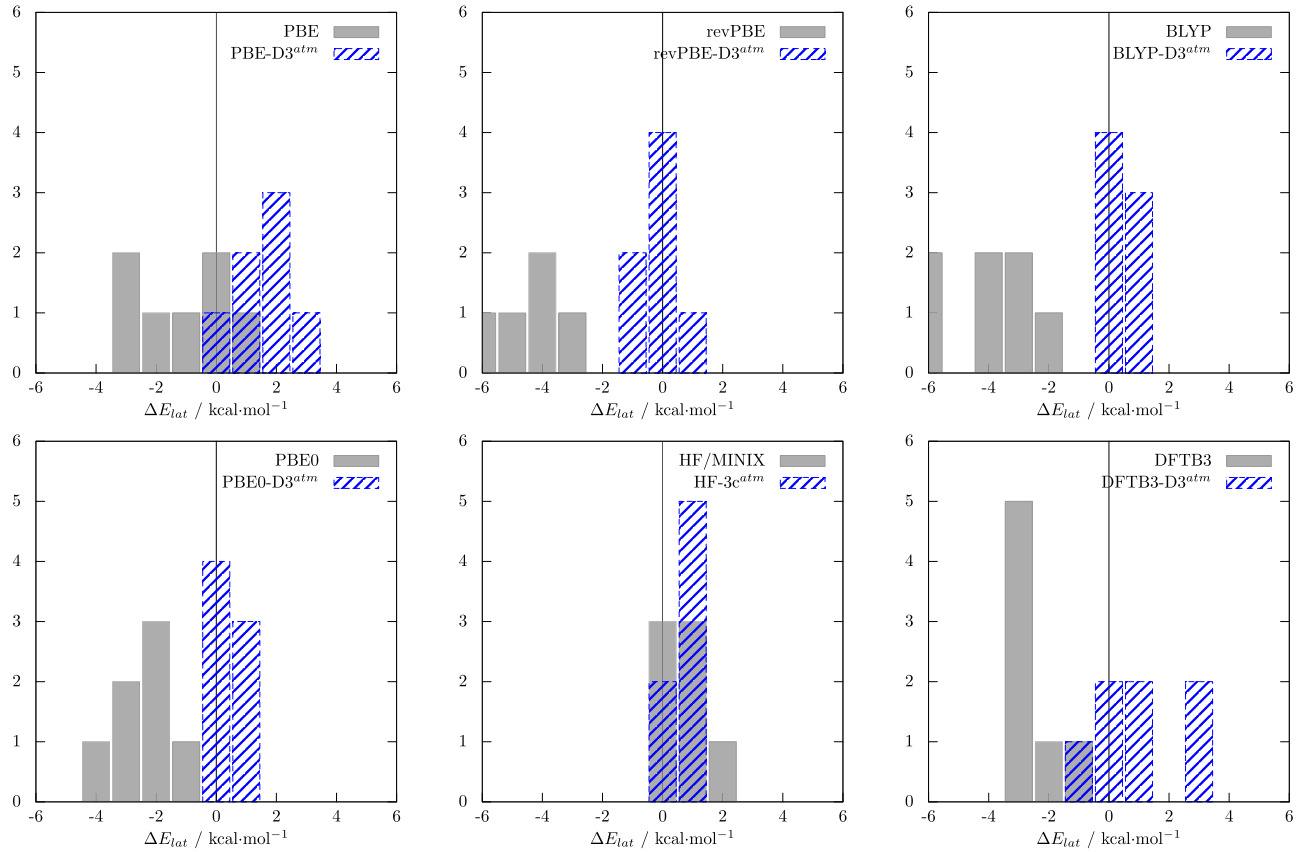

FIG. 5. Deviation of selected methods from the reference lattice energy. Histograms are given with 1 kcal/mol bin width. Error distributions of all functionals are given in the supplementary material.[48]

within 3%. The missing three- and four-center integrals and corresponding empirical pair potentials in the method are especially important for short distances, which explains the bad performance of the tight-binding model for the various high density phases.

Because the unit cell volume as a quality measure could hide systematic error compensations between the different cell dimensions, we additionally investigate the individual cell parameters. The cell data and statistics are given in the supplementary material.[48] The deviations from the references are distributed very uniformly in all directions. The MARDs of the unit cell lengths are approximately 1/3 (to 1/2) of the corresponding unit cell volume MARDs and the ranking of the various methods persists.

TABLE V. Statistical data of the best DFT-D3 methods with other dispersion inclusive DFT methods for the ICE10 lattice energies.

	MD	MAD	RMS[a]
revPBE-D3^{atm}	0.18	0.52	0.65
PBE0-D3^{atm}	0.85	0.85	1.00
PBE + TS[b]	1.92	1.92	0.66
PBE0 + TS[b]	1.16	1.16	1.24
PBE0 + MBD[b]	1.02	1.02	1.12
optPBE-vdW[b]	1.36	1.36	1.36
RPA@PBE[c]	1.63	1.63	1.63

[a]MD, MAD, and root-mean-square deviation (RMS) are given in kcal/mol.
[b]Values take from Ref. 16. Note that only four data points are available.
[c]Values take from Ref. 17. Note that only four data points are available.

C. Electronic lattice energy

We have shown in the last paragraph that London dispersion forces are crucial to get correct cell volumes. The three-body dispersion effects are small but on average improve the results. BLYP-D3^{atm} is the best performing method concerning the structures. However, if one aims at screening of very many structures (polymorphs), the electronic lattice energy is the most important property.

In Table IV, we give the lattice energies of all systems together with the mean deviation (MD) and mean absolute deviation (MAD) in kcal/mol. The statistical data correspond to the seven systems with experimental references. In addition to the previously studied (meta-)GGAs, we show values for the meta-GGA M06L and the hybrid functionals PBE0, B3LYP, and HSE06, which are evaluated at the PBE-D3 geometries. The statistics of selected methods are shown in Figure 5.

Analysis of the energy data supports the trends already observed. Plain PBE is surprisingly good due to error cancellation between the overestimated hydrogen bond energy and missing long-range dispersion. The other plain functionals fail to describe the systems properly. M06L includes to some extend short-range dispersion effects but has an unsatisfactory MAD of 1.6 kcal/mol with a systematic underbinding tendency. Apparently, the correct long range behavior is important in ice. If these contributions are included by the D3(0) scheme, the MAD diminishes to 1.3 kcal/mol and the MD is close to zero. Apart from PBE (which has the intrinsic hydrogen bond errors), all functionals are

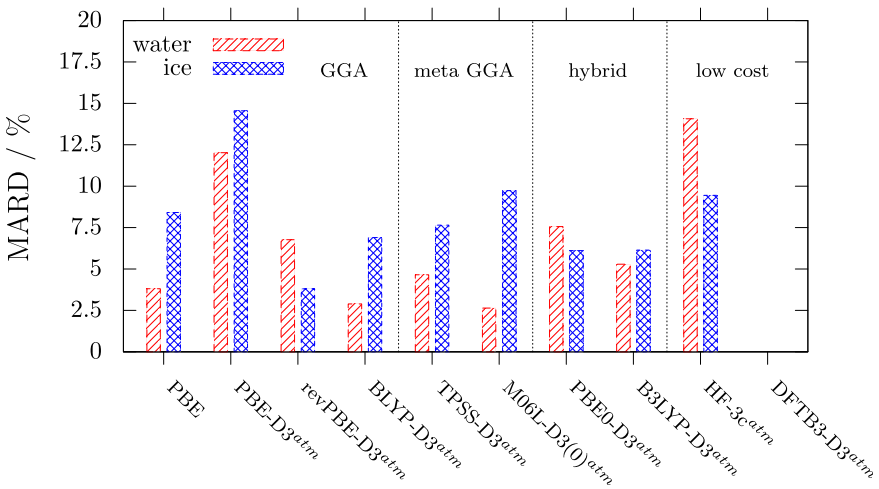

FIG. 6. Performance of various methods for interaction energies of water in the gas and solid state evaluated as MARD on the benchmark sets WATER14 and ICE10.

significantly improved by the dispersion correction. Both revised PBE versions have an exceptionally small MAD of about 0.5 kcal/mol. The effect of the three body dispersion is small, but again its inclusion improves overall the results. The best performing GGA is revPBE-D3^{atm}. It has a tiny MAD of 0.5 kcal/mol, which corresponds to a MARD of 3.8%. BLYP-D3^{atm} also performs well with a MAD of 1 kcal/mol (MARD of 6.9%).

Inclusion of non-local exchange is rather costly in converged basis sets. However, all hybrid functionals have consistently smaller errors compared to their GGA counterparts with MADs usually below 1 kcal/mol. For instance, PBE0-D3^{atm} has a MAD of only 0.8 kcal/mol with MARD of 6.1% which is significantly better than PBE-D3. We use the PBE0-D3^{atm} lattice energies for systems 8-10 shifted by the negative MD on systems 1-7 as best theoretical estimates for these systems where experimental data are lacking. These values should be robust enough to benchmark less accurate small basis DFT, semiempirical, and classical force fields.

The low-cost methods have a larger error spread. Plain B3LYP/6-31G* has a large error of 6 kcal/mol and cannot be recommended. Both HF-3c^{atm} and DFTB3-D3^{atm} are rather good with MADs only slightly above the DFT-D methods (MARD of 9.4% and 11.2%, respectively).

Other dispersion inclusive DFT methods perform very similar, Table V. The TS method[4] is constructed similarly to D3 (use of pre-calculated C_6 coefficients) and can also be applied as a correction to standard density functionals. PBE + TS results in similarly overbound crystals. In combination with PBE0, it is slightly worse compared to PBE0-D3^{atm}. The corresponding many-body dispersion has a similar magnitude as the three-body ATM term and leads to minor improvements; the MAD of PBE0 + MBD is close to 1 kcal/mol. The van der Waals density functional optPBE-vdW includes a non-local kernel combined with an adjusted semi-local DF part. The performance on the ice systems is reasonable, but worse than the DFT-D methods. Also the explicitly correlated RPA method evaluated on PBE orbitals performs worse than DFT-D. This could be significantly improved by replacing PBE with its hybrid variant (including 25%–50% HF exchange) as already recognized by Kresse and coworkers.[17]

D. Comparison to gas phase water clusters

In order to put the above results into a broader perspective, we compare our results to the neutral systems of the WATER27 set compiled by Goddard, dubbed WATER14 in the following.[56] It consists of water oligomers with up to 20 molecules. The reference energies are at the estimated CCSD(T)/CBS level of theory, while for the largest clusters ($20H_2O$), MP2 values are used. Recently, new reference energies at the incremental CCSD(T) level with tighter basis set convergence have been published.[57] Especially for the neutral systems, the deviations are small and we decided to use the original references. In Figure 6, we show the MARDs on both benchmark sets for a selection of methods. The typical functional behaviors are consistently found for both sets. The artificially overly attractive PBE functional leads to the bad performance of PBE-D3^{atm} in both phases. The revised version revPBE-D3^{atm} performs significantly better. BLYP-D3^{atm} is the best performing GGA on the WATER14 set and similar good results are obtained for the solid state with an MARD below 7%. Similarly, both meta-GGAs perform consistently well. Note that for good results with M06L, the correct long-range dispersion contribution by the D3(0) treatment is important. The two hybrid functionals have MARDs between 5% and 7% for both sets. Especially for the gas phase clusters, the low-cost methods show more scatter. HF-3c has a rather large error of 14%, while DFTB3-D3 has a very low error of 5%. These differences are not observed for the ICE10 set where HF-3c and DFTB3-D3 both have a reasonable MARD around 10%, respectively. Despite some differences, a similar performance of the tested methods for both the gas and the solid state is noted. If the DFTB3-D3 value is excluded, the linear correlation coefficient between the gas/solid MARDs of the shown methods is 0.73.

IV. CONCLUSION

We presented a set of ten ice polymorphs ranging from low density (0.9 g/cm^3) to high density (1.5 g/cm^3) phases. The X-ray structural data were back-corrected for zero-point and thermal effects at the HF-3c level in order to get equilibrium structures on the electronic energy surface for convenient

benchmarking. The experimental sublimation energies for seven systems have been extrapolated to 0 K lattice energies by Whalley.[21] On these "experimental" equilibrium geometries and electronic lattice energies, several dispersion inclusive density functional approximations as well as some selected low-cost MO methods were benchmarked.

An accurate treatment of non-local London dispersion interaction is shown to be mandatory for an accurate description of both the structures and energies. All dispersion corrected GGA functionals yield very reasonable structures with MARD from the reference unit cell volume of approximately 2%–3%. The corresponding lattice energies are accurate and close to or below the "chemical accuracy" of 1 kcal/mol. Especially, BLYP-D3^{atm} performs excellently with MARD of the unit cell volumes and MAD of the lattice energy below 1% and 1 kcal/mol, respectively. Compared to corresponding GGAs, the hybrid density functionals improve the lattice energies slightly and can be recommended for obtaining best (routinely) possible energies. While dispersion uncorrected PBE provides reasonable (but not very good) results, the overall picture is more consistent with other (inherently more repulsive) dispersion corrected GGAs. From the investigated low-cost methods, we recommend HF-3c for geometry optimization including frequency calculations. This conclusion is in agreement with the good performance of HF-3c for noncovalently bound organic complexes and solids.[7] For an analysis of the individual non-covalent interaction terms and their compensations in dispersion-corrected minimal basis set HF calculations, see Ref. 42. The structures of the tight-binding model DFTB3-D3 have to be taken with care. The lattice energies at this level are rather good, especially when considering the tremendous speed up of approximately 2-3 orders of magnitude compared to full DFT calculations.

In summary, we have shown a hierarchy of methods which is ideally suited to describe ice at various densities. Some comparisons with water clusters furthermore indicate that the conclusions are transferable to the liquid state where detailed benchmarking studies are hampered by the sampling problem. With the best performing theoretical models, also, e.g., large solid water interfaces should be described quantitatively. Especially, the cheaper methods can be used in molecular dynamic simulations, where full DFT calculations are often prohibitive in terms of computational cost.

ACKNOWLEDGMENTS

The authors thank Christoph Bannwarth for helpful discussions.

[1]R. G. Parr and W. Yang, *Density-Functional Theory of Atoms and Molecules* (Oxford University Press, Oxford, 1989); W. Koch and M. C. Holthausen, *A Chemist's Guide to Density Functional Theory* (Wiley-VCH, New York, 2001); J. Dreizler and E. K. U. Gross, *Density Functional Theory, An Approach to the Quantum Many-Body Problem* (Springer, Berlin, 1990); R. Paverati and D. G. Truhlar, Philos. Trans. R. Soc. A **372**, 20120476 (2014); A. Ruzsinszky and J. P. Perdew, Comput. Theor. Chem. **963**, 2 (2011).

[2]S. Kristyán and P. Pulay, Chem. Phys. Lett. **229**, 175 (1994); J. M. Pérez-Jordá and A. D. Becke, *ibid.* **233**, 134 (1995); P. Hobza, J. Sponer, and T. Reschel, J. Comput. Chem. **16**, 1315 (1995); M. Allen and D. J. Tozer, J. Chem. Phys. **117**, 11113 (2002).

[3]S. Grimme, J. Antony, S. Ehrlich, and H. Krieg, J. Chem. Phys. **132**, 154104 (2010).

[4]A. Tkatchenko and M. Scheffler, Phys. Rev. Lett. **102**, 073005 (2009); A. Tkatchenko, R. A. DiStasio, R. Car, and M. Scheffler, *ibid.* **108**, 236402 (2012).

[5]A. D. Becke and E. R. Johnson, J. Chem. Phys. **123**, 154101 (2005); O. A. Vydrov and T. Van Voorhis, *ibid.* **133**, 244103 (2010).

[6]K. E. Riley, M. Pitoňák, P. Jurečka, and P. Hobza, Chem. Rev. **110**, 5023 (2010); S. Grimme, WIREs Comput. Mol. Sci. **1**, 211 (2011).

[7]J. G. Brandenburg, M. Hochheim, T. Bredow, and S. Grimme, J. Phys. Chem. Lett. **5**, 4275 (2014).

[8]T. Bartels-Rausch, V. Bergeron, J. H. E. Cartwright, R. Escribano, J. L. Finney, H. Grothe, P. J. Gutirrez, J. Haapala, W. F. Kuhs, J. B. C. Pettersson, S. D. Price, C. I. Sainz-Daz, D. J. Stokes, G. Strazzulla, E. S. Thomson, H. Trinks, and N. Uras-Aytemiz, Rev. Mod. Phys. **84**, 885 (2012).

[9]D. A. Palmer, R. Fernández-Prini, and A. H. Harvey, *Aqueous Systems at Elevated Temperatures and Pressure* (Academic Press, London, 2004).

[10]M. D. Ben, J. Hutter, and J. VandeVondele, J. Chem. Theory Comput. **9**, 2654 (2013); M. D. Ben, M. Schoenherr, J. Hutter, and J. VandeVondele, J. Phys. Chem. Lett. **4**, 3753 (2013).

[11]J. Carrasco, A. Hodgson, and A. Michaelides, Nat. Mater. **11**, 667 (2012); S. Chutia, M. Rossi, and V. Blum, J. Phys. Chem. B **116**, 14788 (2012); R. A. DiStasio, B. Santra, Z. Li, X. Wu, and R. Car, J. Chem. Phys. **141**, 084502 (2014).

[12]E. G. Hohenstein and C. D. Sherrill, WIREs Comput. Mol. Sci. **2**, 304 (2012).

[13]L. Goerigk and S. Grimme, J. Chem. Theory Comput. **7**, 291 (2011).

[14]S. Grimme and M. Steinmetz, Phys. Chem. Chem. Phys. **15**, 16031 (2013).

[15]A. O. de-la Roza and E. R. Johnson, J. Chem. Phys. **137**, 054103 (2012); A. M. Reilly and A. Tkatchenko, *ibid.* **139**, 024705 (2013).

[16]B. Santra, J. Klimeš, A. Tkatchenko, D. Alfè, B. Slater, A. Michaelides, R. Car, and M. Scheffler, J. Chem. Phys. **139**, 154702 (2013); O. Kambara, K. Takahashi, M. Hayashi, and J.-L. Kuo, Phys. Chem. Chem. Phys. **14**, 11484 (2012).

[17]M. Macher, J. Klimeš, C. Franchini, and G. Kresse, J. Chem. Phys. **140**, 084502 (2014); M. J. Gillan, D. Alfè, P. J. Bygrave, C. R. Taylor, and F. R. Manby, *ibid.* **139**, 114101 (2013).

[18]T. Takamuku, K. Saisho, S. Nozawa, and T. Yamaguchi, J. Mol. Liq. **119**, 122 (2005).

[19]P. V. Hobbs, *Ice Physics* (Oxford University Press, New York, 1974); C. Vega, C. McBride, E. Sanz, and J. L. F. Abascal, Phys. Chem. Chem. Phys. **7**, 1450 (2005).

[20]A. D. Fortes, I. G. Wood, M. Alfredsson, L. Vocadlo, and K. S. Knight, J. Appl. Cryst. **38**, 612 (2005); C. Lobban, J. L. Finney, and W. F. Kuhs, J. Chem. Phys. **117**, 3928 (2002).

[21]E. Whalley, J. Chem. Phys. **81**, 4087 (1984).

[22]B. Kamb, Science **150**, 205 (1965).

[23]Y. Yoshimura, S. T. Stewart, M. Somayazulu, H.-k. Mao, and R. J. Hemley, J. Chem. Phys **124**, 024502 (2006); J. D. Jorgensen, R. A. Beyerlein, N. Watanabe, and T. G. Worlton, J. Chem. Phys. **81**, 3211 (1984).

[24]J. D. Londono, W. F. Kuhs, and J. L. Finney, J. Chem. Phys. **98**, 4878 (1993); S. J. La Placa, W. C. Hamilton, B. Kamb, and A. Prakash, *ibid.* **58**, 567 (1973).

[25]C. G. Salzmann, P. G. Radaelli, A. Hallbrucker, E. Mayer, and J. L. Finney, Science **311**, 1758 (2006).

[26]C. G. Salzmann, P. G. Radaelli, E. Mayer, and J. L. Finney, Phys. Rev. Lett. **103**, 105701 (2009).

[27]G. Kresse and J. Furthmüller, J. Comput. Mat. Sci. **6**, 15 (1996); Phys. Rev. B **54**, 11169 (1996).

[28]P. E. Blöchl, Phys. Rev. B **50**, 17953 (1994); G. Kresse and D. Joubert, *ibid.* **59**, 1758 (1999).

[29]J. G. Brandenburg, S. Grimme, P. G. Jones, G. Markopoulos, H. Hopf, M. K. Cyranski, and D. Kuck, Chem. - Eur. J. **32**, 6745 (2013).

[30]J. P. Perdew, K. Burke, and M. Ernzerhof, Phys. Rev. Lett. **77**, 3865 (1996); erratum, **78**, 1396 (1997).

[31]B. Hammer, L. B. Hansen, and J. K. Norskov, Phys. Rev. B **59**, 7413 (1999).

[32]Y. Zhang and W. Yang, Phys. Rev. Lett. **80**, 890 (1998).

[33]A. D. Becke, Phys. Rev. A **38**, 3098 (1988); C. Lee, W. Yang, and R. G. Parr, Phys. Rev. B **37**, 785 (1988).

[34]J. Tao, J. P. Perdew, V. N. Staroverov, and G. E. Scuseria, Phys. Rev. Lett. **91**, 146401 (2003).

[35]Y. Zhao and D. G. Truhlar, J. Chem. Phys. **125**, 194101 (2006).
[36]C. Adamo and V. Barone, J. Chem. Phys. **110**, 6158 (1999).
[37]A. D. Becke, J. Chem. Phys. **98**, 5648 (1993); P. J. Stephens, F. J. Devlin, C. F. Chabalowski, and M. J. Frisch, J. Phys. Chem. **98**, 11623 (1994).
[38]A. V. Krukau, O. A. Vydrov, A. F. Izmaylov, and G. E. Scuseria, J. Chem. Phys. **125**, 224106 (2006).
[39]S. Grimme, S. Ehrlich, and L. Goerigk, J. Comput. Chem. **32**, 1456 (2011).
[40]B. M. Axilrod and E. Teller, J. Chem. Phys. **11**, 299 (1943); Y. Muto, Proc. Phys. Math. Soc. Jpn. **17**, 629 (1944).
[41]R. Dovesi, R. Orlando, A. Erba, C. M. Zicovich-Wilson, B. Civalleri, S. Casassa, L. Maschio, M. Ferrabone, M. De La Pierre, P. D'Arco, Y. Noël, M. Causà, M. Rérat, and B. Kirtman, Int. J. Quantum Chem. **114**, 1287 (2014).
[42]H. Kruse and S. Grimme, J. Chem. Phys. **136**, 154101 (2012); J. G. Brandenburg, M. Alessio, B. Civalleri, M. F. Peintinger, T. Bredow, and S. Grimme, J. Phys. Chem. A **117**, 9282 (2013).
[43]R. Sure and S. Grimme, J. Comput. Chem. **34**, 1672 (2013); J. G. Brandenburg and S. Grimme, Top. Curr. Chem. **345**, 1 (2014).
[44]M. Elstner, D. Porezag, G. Jungnickel, J. Elsner, M. Haugk, T. Frauenheim, S. Suhai, and G. Seifert, Phys. Rev. B **58**, 7260 (1998).
[45]J. G. Brandenburg and S. Grimme, J. Phys. Chem. Lett. **5**, 1785 (2014).
[46]B. Aradi, B. Hourahine, and T. Frauenheim, J. Phys. Chem. A **111**, 5678 (2007); M. Elstner, *ibid.* **111**, 5614 (2007).
[47]M. Gaus, A. Goez, and M. Elstner, J. Chem. Theory Comput. **9**, 338 (2013).
[48]See supplementary material at http://dx.doi.org/10.1063/1.4916070 for explicit k-point grid utilized in all calculations, unit cell parameters and lattice energies of all tested method combinations, explicit error distributions, and optimized geometries at the PBE-D3/1000 eV level.
[49]J. G. Brandenburg and S. Grimme, Theor. Chem. Acc. **132**, 1399 (2013).
[50]B. Santra, J. c. v. Klimeš, D. Alfè, A. Tkatchenko, B. Slater, A. Michaelides, R. Car, and M. Scheffler, Phys. Rev. Lett. **107**, 185701 (2011).
[51]E. D. Murray and G. Galli, Phys. Rev. Lett. **108**, 105502 (2012).
[52]L. Goerigk, H. Kruse, and S. Grimme, ChemPhysChem **12**, 3421 (2011).
[53]J. P. Perdew, K. Burke, and M. Ernzerhof, Phys. Rev. Lett. **80**, 891 (1998); J. Moellmann and S. Grimme, J. Phys. Chem. C **118**, 7615 (2014).
[54]M. Del Ben, M. Schönherr, J. Hutter, and J. VandeVondele, J. Phys. Chem. Lett. **4**, 3753 (2013); K. Forster-Tonigold and A. Gro, J. Chem. Phys. **141**, 064501 (2014).
[55]H. Kruse, L. Goerigk, and S. Grimme, J. Org. Chem. **77**, 10824 (2012).
[56]V. S. Bryantsev, M. S. Diallo, A. C. T. van Duin, and W. A. Goddard, J. Chem. Theory Comput. **5**, 1016 (2009).
[57]T. Anacker and J. Friedrich, J. Comput. Chem. **35**, 634 (2014).